Enhanced Photostability of a Ruthenium(II) Polypyridyl Complex under Highly Oxidizing Aqueous Conditions by its Partial Inclusion into a Cyclodextrin

Pau Farras[a,b]*, Helen Waller[c] and Andrew C. Benniston[a]*

Abstract: The complex $[Ru(bpy)_2L]^{2+}$, where bpy = 2,2'-bipyridine, L = 4-(phenylethynyl)-2,2'-bipyridine, was prepared in its racemic and resolved forms (Δ and Λ). The phenylethynyl unit on the bipyridine for the complex acts as a binding site for α-cyclodextrin in water (1:1 complex, K = 3390 M^{-1}) or β-cyclodextrin (2:1 complex, K_1 = 887 M^{-1}, K_2 = 8070 M^{-1}). The presence of the cyclodextrin provides partial protection to the complex under light-activated water oxidation conditions.

Introduction

Ruthenium(II) polypyridyl complexes have been widely studied over the last few decades in dye-sensitized solar cells (DSSC), due to their favorable photoelectrochemical properties and high stability in the oxidized state.[1,2] Several literature examples are known where diverse types of ligands have helped tune their properties and improve the efficiency of the solar cells.[3] Strategies have also been developed to improve the stability of the systems including the use of additives and, most important, the use of non-aqueous solvents.[4] On the other hand, the number of cases is certainly less where ruthenium dyes are used in dye-sensitized photoelectrochemical cells (DSPECs) for performing the demanding water oxidation reaction.[5] The two most widely used dyes are the simple $[Ru(bpy)_3]^{2+}$ (bpy = 2,2'-bipyridine) and its phosphonated derivative, $[Ru(4,4'\text{-}PO_3H_2\text{-}bpy)(bpy)_2]^{2+}$.[6] One main reason for the lack of examples can be attributed to the low oxidation potentials of most ruthenium(II) dyes used in DSPECs, which are not high enough to charge up a suitable catalyst capable of driving the highly demanding water oxidation reaction, $E^0(O_2/H_2O)$ = 1.23 – 0.059 x pH vs. NHE.[7] The first step towards the construction of a water splitting device is the study of each of the individual half-reactions; the oxidation of water to oxygen being the most complicated from a mechanistic viewpoint. Hence, the homogeneous photo-oxidation of water has been studied in great detail to try and understand the processes occurring during the reaction.[8] A suitable photosensitizer for water oxidation must have strong absorbance in the visible spectrum, a long excited state lifetime at room temperature, enough photostability under aqueous environments and a high oxidation potential (high enough to oxidize the water oxidation catalyst). In three-component systems composed of a photosensitizer (PS), a water oxidation catalyst (WOC) and a sacrificial electron acceptor (SEA), only $[Ru(bpy)_3]^{2+}$, $[Ru(4,4'\text{-}CO_2H\text{-}bpy)(bpy)_2]^{2+}$ and the tetranuclear $[Ru\{(\mu\text{-}dpp)Ru(bpy)_2\}_3]^{8+}$, (dpp = 2,3-bis(2′-pyridyl)pyrazine) have, so far, demonstrated some of these requirements. Recently, we have shown that Bodipy-ruthenium(II) polypyridyl dyad photosensitizers could meet some of the requirements for light-driven water oxidation, although the described system was only able to oxidize organic substrates.[9] A common problem with photosensitizers in aqueous solution is their low photostability because of degradation. Answers to the problem have included using acidic pH or weakly nucleophilic inorganic buffer systems instead of the most common phosphate buffer.[10] For any practical device overcoming the photostability problem in water is imperative.

For a while it has been recognized that the properties of organic dyes can be improved by molecular encapsulation.[11] Host-guest systems, or the protection of dyes inside inorganic cavities, has opened up new avenues of research that would have not been possible because of fast dye photodegradation. Among the plethora of guests, cyclodextrins (CDs) stand out because of their ability to incorporate aromatic molecules within the macrocyclic cavity.[12] One of the earliest examples of dye encapsulation inside a CD was a report by Cramer and co-workers who described the inclusion of an azo dye within the cavity of α-CD.[13] Various examples can also be found where CDs form host-guest structures with electron relays that help stabilize intermediate photoproducts against back-electron-transfer reactions, in particular when using methyl viologen derivatives.[14] The use of CDs for localizing metal-based molecular complexes is less established and zeolites are the preferred choice for their encapsulation.[15]

In this work, we have studied the combination of the molecular encapsulation of a specifically designed ruthenium dye by a CD, with the aim of enhancing its photostability under the harsh conditions of light-driven water oxidation. A recent report by Sun *et al.*[16] highlighted how binding of the water oxidation catalyst to a cyclodextrin appended to the photosensitizer enhanced the turnover number for oxygen production. However, the covalent

[a] Dr P. Farras and Prof A. C. Benniston
Molecular Photonics Laboratory
School of Chemistry
Newcastle University
Newcastle upon Tyne, NE1 7RU, UK
E-mail: pau.farras@ncl.ac.uk; a.c.benniston@ncl.ac.uk
[b] Dr P. Farras
School of Chemistry
NUI Galway
Galway, Ireland
[c] Dr H. Waller
Institute for Cell and Molecular Biosciences, Medical School
Newcastle University
Newcastle upon Tyne, NE2 4HH, UK

attachment of the cyclodextrin to the photosensitzer adds extra synthetic difficulties to the system. On the other hand, in the present paper, the complex consists of a basic $[Ru(bpy)_2L]^{2+}$ core, where L is a mono-substituted 2,2'-bipyridine with a phenylethynyl unit. One specific design feature is the presence of the triple bond to a single bipyridine unit.[17] The lowering of the reduction potential for this ligand promotes selective electron migration to it upon formation of the excited triplet metal-to-ligand charge transfer (^{3}MLCT) state.[18] Hence, a unique site is introduced for quenching by an oxidizing agent (Scheme 1 right). The water oxidation catalyst can be charged up from the generated Ru^{3+} centre. Mechanisms for degradation of Rubpy complexes include aquation by loss of a single bipy ligand and hydroxide attack at the α-carbon of a pyridine subunit.[19] In a homoleptic Rubpy complex the ligands are all equivalent and so there is no preference for which one is removed or modified. For a heteroleptic Rubpy complex the easier to reduce ligand is more prone to side reactions since most electron density is focused at a single site. We hypothesized that protection of the unique ligand in the complex would enhance photostability provided that the initial quenching pathway was not affected by the presence of the CD (Scheme 1 left). Since mono-nuclear Rubpy complexes are also chiral (Δ and Λ forms) and a solution is thus racemic, we wanted to remove any potential complication for the ^{1}H NMR binding studies, and determine if there was some preferential binding to CDs. Thus, the starting synthons Δ- and Λ-$[Ru(bpy)_2(py)_2]^{2+}$ were employed to prepare chirally pure photosensitizers.[20]

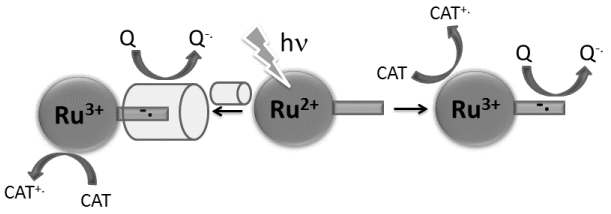

Scheme 1. Right: basic mechanism for photoactivation of a ruthenium-based sensitizer in the presence of a quencher (Q) and water oxidation catalyst (CAT). Left: the same process with an added CD to encapsulate the appended phenylacetylene unit.

Results and Discussion

Molecular Synthesis

The synthesis of the ruthenium dye **rac-2** is shown in Scheme 2, highlighting two slightly different routes to the desired compound. The first pathway consisted of the synthesis of **rac-1** using the classical procedure of reacting 4-bromo-2,2'-bipyridine with stoichiometric amounts of the precursor $[Ru(bpy)_2Cl_2]$.[21] A Sonogashira cross-coupling reaction of **rac-1** with phenylacetylene afforded the dye **rac-2** in a moderate yield. The second route involved the synthesis of 4-(phenylethynyl)-2,2'-bipyridine (Ph-E-bpy), following by its complexation with $[Ru(bpy)_2Cl_2]$ to obtain the dye **rac-2** in a slightly higher yield. The optically pure ruthenium complexes **Δ-1**, **Λ-1**, **Δ-2** and **Λ-2** were prepared in a single step by treatment of the resolved ruthenium complexes Δ- and Λ-$[Ru(bpy)_2py_2]$[dibenzoyltartrate-O,O'] with the appropriate chelating ligands in ethylene glycol for 4 hours. Moreover, dyes **Δ-2** and **Λ-2** were also obtained optically pure starting from **Δ-1** and **Λ-1**, respectively, and following the same reactions conditions as described for the racemic mixture (*vide supra*). This is of interest, especially because several groups are currently interested in the polymetallic assembly involving optically pure ruthenium complexes as individual components.[22] Dyes **Δ-1** and **Λ-1** are easily synthesized and could be useful starting materials for more complex systems, while maintaining their optical purity. All complexes were isolated as the hexafluorophosphate salts by column chromatography or preparative thin layer chromatography, and were obtained as microcrystalline solids in good yields. Their molecular structures were unambiguously assigned by using ^{1}H, ^{13}C and 2D homo- and heteronuclear NMR spectroscopy, electrospray mass spectrometry and elemental analysis (the synthesis of rac-**1** has been reported previously).[23] Both dyes analyzed by ESI-MS gave an intense molecular peak with the expected isotopic profile corresponding to the loss of two PF_6^- counter anions assigned to a doubly charged species, and the expected profile for the singly charged species corresponding to the loss of one PF_6^- anion. The absolute configurations of Δ-**1** and Λ-**1**, and Δ-**2** and Λ-**2** were assigned by circular dichroism using the characteristic bpy-based π–π^* absorption band at λ_{max} = 287 nm (see Supporting Information). The $[\alpha]_D$ values of the complexes were recorded in acetonitrile with $[\alpha]_D$ = -425 (c = 0.4 mM, CH_3CN) for Δ–**1**, $[\alpha]_D$ = 483 (c = 0.5 mM, CH_3CN) for Λ–**1**, $[\alpha]_D$ = -680 (c = 0.4 mM, CH_3CN) for Δ–**2** and $[\alpha]_D$ = 620 (c = 0.5 mM, CH_3CN) for Λ–**2**.

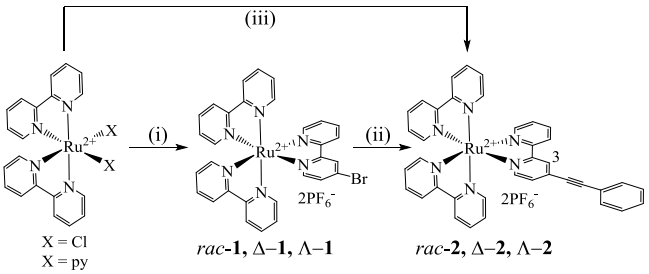

Scheme 2. Reagents and conditions: i) 4-bromo-bipyridine, EtOH/H_2O, reflux, 4 h, NH_4PF_6(aq), 80%; ii) phenylacetylene (2 eq.), diisopropylamine (10 eq.), 5% $[PdCl_2(PPh_3)_2]$, 10% CuI, THF, 18 h at rt, then 3 h reflux, NH_4PF_6(aq), 68%; (iii) 4-(phenylethynyl)-bipyridine, EtOH/H_2O, reflux, 4 h, NH_4PF_6(aq), 75%.

NMR Spectroscopy and Mass Spectrometry Studies

To all intents and purposes the ^{1}H and ^{13}C NMR spectra for **Δ-1** and **Λ-1** were the same as described for the racemic compound **rac-1**.[23] The spectra of **rac-2**, **Δ-2** and **Λ-2** in acetonitrile were identical, and displayed resonances at 8.50, 8.06, 7.72 and 7.41 ppm corresponding to protons of the unsubstituted bipyridine ligands. The remaining proton resonances could be assigned to the Ph-E-bpy ligand because of the chemical shift and integrals. A comparison of NMR spectra for **rac-1** and **rac-2** shows an upfield shift for proton H_3 from 8.72 to 8.61 ppm due to the presence of the phenylethynyl unit, while the remaining peaks

appear at very similar chemical shifts (see Supporting Information). We were interested to see the effect of any interaction between α-cyclodextrin (α–CD) and **rac-2**, **Δ-2** and **Λ-2**. As hypothesized, the "arm-like" structure for **rac-2** would fit within the cavity of the α-CD and form a host-guest structure. The observation of proton chemical shift differences between the free guest/host and the complex is the simplest NMR experiment to monitor complexation. Demarco *et al.* studied CD complexes by observing the chemical shifts changes (Δδ) of protons H_{CD3} and H_{CD5} inside the cavity of α-CD when in presence of aromatic molecules due to the anisotropic effect of the aromatic ring.[24] Greatbanks *et al.* concluded that when $\Delta\delta(H_{CD3}) > \Delta\delta(H_{CD5})$, partial inclusion of the guest inside the cavity occurs and when $\Delta\delta(H_{CD3}) < \Delta\delta(H_{CD5})$ a total inclusion takes place.[25] First tests involved the use of **rac-2** and titration of incremental amounts of α-CD in a 50% CD_3CN/D_2O mixture to completely dissolve **rac-2**. No chemical shift changes were observed, most probably due to the formation of an inclusion complex between α-CD and acetonitrile, as previously observed in the literature.[26] Therefore, experiments were conducted exclusively in D_2O. Changes in a majority of the aromatic proton chemical shifts for **rac-2** in the presence of α-CD are clear and are shown in the Supporting Information. Moreover, peaks corresponding to H_{CD3} and H_{CD5} from α-CD are shifted downfield with $\Delta\delta(H_{CD3})$ = 0.065 ppm and $\Delta\delta(H_{CD5})$ = 0.072 ppm, indicating a total inclusion of the phenylethynyl unit inside the cavity.

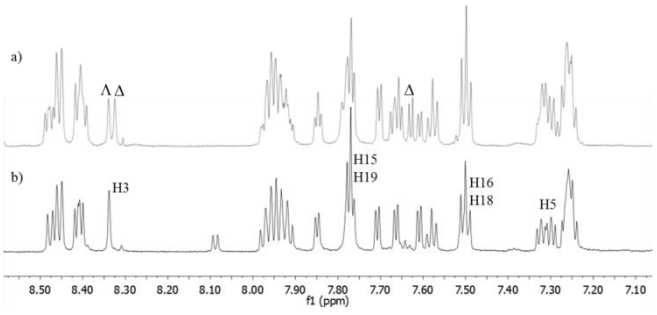

Figure 1. ^{1}H NMR spectra of a) rac-**2** + 10 equiv. of α–CD and b) Λ-**2** + 10 equiv. of α-CD in D_2O (700 MHz, 298 K). Labelled protons have a ROESY interaction with α-CD (see Figure 2 for number labelling of molecular components).

An especially attractive feature of cyclodextrins is their ability to act as chiral shift reagents, and several examples are known where racemic mixtures of ruthenium complexes were separated by their application to solutions.[27] In our case, separation of a racemic mixture was not required, because two pure enantiomers were already on hand. However, we wanted to observe if α-CD would be a good chiral shift agent for rac-**2**, and more importantly if the **Δ-2** and **Λ-2** enantiomers would display subtle ^{1}H shifts upon host-guest complexation. Indeed, the chemical environment for H_3 is subtlety different for the two enantiomers in the presence of α–CD (Figure 1). Other peaks also underwent a chemical shift change, but it was problematic to assign the entire spectrum for the **Δ-2** enantiomer. The 2D ROESY spectrum of the **Λ-2** and α-CD mixture in D_2O afforded compelling evidence for which hydrogen atoms from the ruthenium complex were characteristic of the host-guest interaction (Figure 1 and Figure 2). The correlation between protons corresponding to the Ph-*E*-bpy ligand with hydrogen atoms H_{CD3}, H_{CD5} and H_{CD6} from α–CD demonstrate the inclusion of phenylethynyl unit, and also gives indication on the mode and depth of penetration of the guest. Full assignment of the ^{1}H NMR spectrum of the **Λ-2**:α–CD complex was achieved using standard 2D experiments (see Supporting Information).

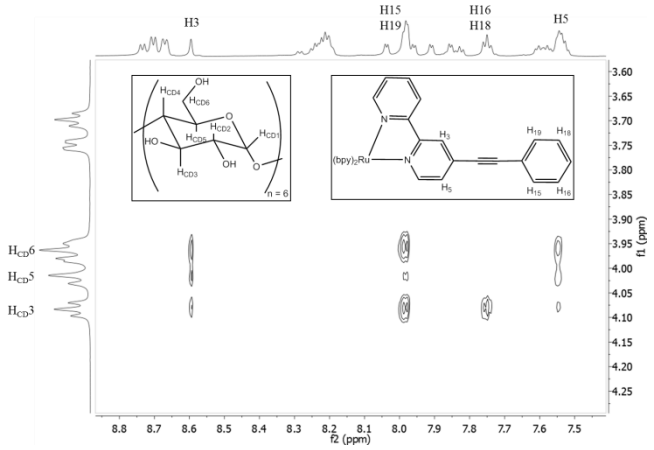

Figure 2. 2D ROESY spectrum of the mixture of **Λ-2b** and α-CD (10 equiv.). at 700 MHz in D_2O, T = 323 K.

Further confirmation that **rac-2** and α–CD formed a host-guest supramolecular complex was obtained by mass spectrometry using a D_2O sample from the NMR measurements. First, the NMR sample was extracted with dichloromethane to remove **rac-2** and both solvents were then evaporated *in vacuo*. The two separate samples redissolved in water were analyzed by ESI-MS. The mass spectrum from the dichloromethane extract contained only peaks associated with **rac-2** at *m/z* = 335.0565 $(M\text{-}2PF_6)^{2+}$ and 815.0922 $(M\text{-}PF_6)^+$. In contrast, the other sample showed an additional peak at *m/z* = 821.2282 corresponding to the supramolecular complex **rac-2**:α–CD. Additional peaks in the mass spectrum were also observed for the free α-CD since this was used in excess in the NMR experiments.

Isothermal Calorimetry

To assess the cooperative factor of the binding process, we proved the interaction between **Λ-2** and α–CD using isothermal titration calorimetry (ITC) experiments. The chirally pure isomer was used to avoid any potential complications due to the racemic mixture. In addition, the **Λ-2** counter anion was substituted from PF_6^- to NO_3^- by anion exchange to increase its solubility in water.

A typical ITC titration curve corresponding to the binding interaction of **Λ-2** and α-CD is represented in Figure 3. Heat released after successive injections of 2 μL aliquots of cyclodextrin into a solution of **Λ-2** were integrated and expressed as a function of the molar ratio between the two reactants. Data were corrected for dilution effects to afford a clear differential binding curve. The least-squares best fit to the binding curve was obtained by using a standard one-site binding model (1:1) leading to the direct determination of the stoichiometry of the interaction (N = 1.09 ± 0.01), binding constant ($K_{average}$ = 3390 M^{-1}) and the enthalpy associated with the interaction between **Λ-2** and α–CD ($\Delta H_{average}$ = -946 cal mol^{-1}). A similar binding experiment was repeated for β-CD to ascertain binding parameters for **Λ-2**, and assess any potential cavity size effect. Interestingly, a 1:1 best fit showed a different stoichiometry for the process (N = 0.49), which represents a binding of two **Λ-2** per molecule of β-CD (see Supporting Information for more details). A re-analysis of the data for a 2:1 complex afforded parameters to the best fit of K_1 = 887 M^{-1} (ΔH = -532 cal mol^{-1}) and K_2 = 8070 M^{-1} (ΔH = +504 cal mol^{-1}). The cavity for β-CD appears to be consummate for binding two phenylethynyl groups of a bipyridine ligand, possibly facilitated by π–π-stacking within the cyclodextrin cavity.

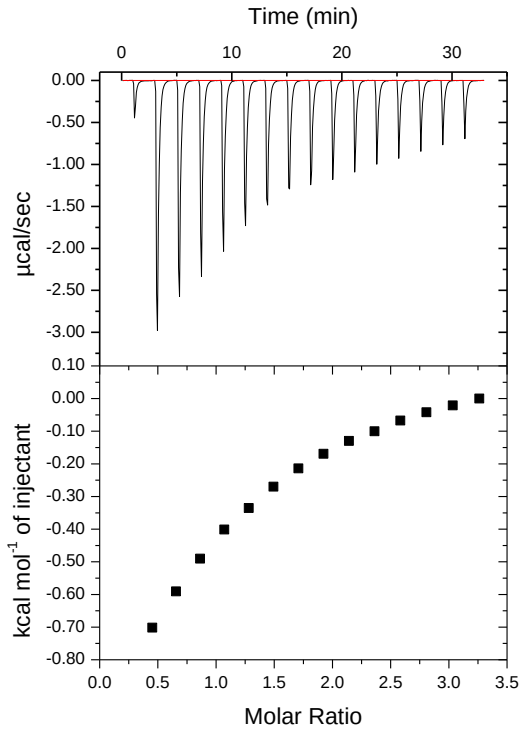

Figure 3. Isothermal titration calorimetric curve for the interaction of Λ-2 (1.14 mM) with α-CD (22.8 mM) in phosphate buffer solutions (pH = 7.1) at 298 K. The top panel show the raw data of the titration, and the bottom panel show the normalized integrated peaks against molar ratio (squared symbols). All the data points were corrected for the heat of dilution.

Electrochemical and Photophysical Characterization

The basic photophysical properties of the ruthenium sensitizer **rac-2** are summarized in Table 1, and are compared with **rac-1** and other similar compounds. Cyclic voltammograms and absorption and emission spectra can be found in the Supporting Information. The redox properties of **rac-2** are very similar to the other compounds shown in Table 1 and are dominated by a reversible oxidation peak at 1.52 V ($Ru^{III/II}$) and three reduction peaks at -1.01, -1.27 and -1.51 V. By comparison with the parent $[Ru(bpy)_3]^{2+}$, it is possible to assign the peak at -1.01 V to the substituted ligand Ph-E-bpy, which is easier to reduce due to the electron-withdrawing properties of the phenylethynyl unit. This corroborates the design strategy that places the excited electron upon irradiation into the arm-like ligand. Interestingly, the oxidation potential for **rac-2** is 20 mV higher than $[Ru(bpy)_3]^{2+}$, which makes it a feasible sensitizer for the photooxidation of water.

Table 1. Electrochemical and photophysical properties of **rac-1** and **rac-2** and similar ruthenium(II) sensitizers.

sensitizer	λ_{abs}, nm (ε, M^{-1} cm^{-1})[a]	λ_{PL} (nm)[b]	Φ_{PL} (10^{-2})	$E_{1/2,ox}$ (V)[c]	$E_{1/2,red}$ (V)[c]
$[Ru(bpy)_2(Br\text{-}bpy)]^{2+}$ (**1**)[d]	452 (14,000)	613	5.6	1.53	-1.00 (irr), -1.12, -1.29, -1.54
$[Ru(bpy)_2(Ph\text{-}E\text{-}bpy)]^{2+}$ (**2**)	458 (16,000)	619	6.8	1.52	-1.01, -1.27, -1.51
$[Ru(bpy)_3]^{2+}$[e]	452 (16,000)	626	5.9	1.50	-1.10, -1.27, -1.54
$[Ru(Ph\text{-}E\text{-}bpy)_3]^{2+}$[f]	468 (16,000)	605	13.0	1.67	-0.92, -1.08

[a] Measurements were made at 298 °K. The molar extinction coefficients, ε, were obtained from CH_3CN solutions. [b] Photoluminescence maximum, uncorrected for detector response. All data were obtained from aerated CH_3CN solutions. [c] Half-wave potentials were measured at a glassy carbon working electrode in 0.1 M $TBAPF_6/CH_3CN$ solution using SSCE as reference. Data are reported *vs.* NHE. [d] In agreement with literature data, reference 28. [e] Reference 29. [f] Reference 30.

The UV/visible absorption bands of **rac-2** are typical of Ru(bpy)-type complexes, with an intense UV absorption band (λ_{max} = 287 nm), attributed to ligand-centered π– π* transitions, and a visible light absorption band (λ_{max} = 458 nm), attributed to metal-to-ligand charge transfer (MLCT). The emission spectrum for rac-**2** is consistent with the other complexes, and the greater luminescence quantum yield, 6.8% *vs*. 5.6% respectively, is due to the presence of the phenylethynyl unit; also observed for the homotopic complex $[Ru(Ph\text{-}E\text{-}bpy)_3]^{2+}$.[30]

Stern-Volmer Quenching

Within the proposed model illustrated in Scheme 1 quenching of the complex excited state by Q results in the generation of the Ru(III) metal centre. The Stern-Volmer quenching of photoexcited $[Ru(bpy)_3]^{2+}$ by persulfate ($S_2O_8^{2-}$) as the quencher is slightly complicated because of the formation of a ground state ion-pair complex.[31] The equilibrium constant (K_{IP}) for its formation is ionic strength dependent, and in water has been reported to be << 10 M^{-1}, and as a consequence the standard Stern-Volmer quenching model is appropriate at low concentrations of $S_2O_8^{2-}$. It was assumed that K_{IP} would be very similar for free **rac-2** and $S_2O_8^{2-}$ in water at low concentrations. The complication envisaged for the host-guest assembly of **rac-2** with α-CD was that quenching would be inefficient because of a potential steric hindrance effect. That is, the $S_2O_8^{2-}$ would not get in close enough contact to the substituted bipyridine ligand to facilitate electron transfer. In an attempt to investigate this potential steric complication, Stern-Volmer measurements were performed on a water solution of **rac-2** (pH 7, c = 10 μM) in the presence of 0, 10 and a 100-fold excess of α-CD (see Supporting Information). The feasibility of working at much higher concentrations of **rac-2** is hampered by potential inner-filter effects for the luminescence measurements. As a result, given the binding constant derived by ITC experiments, the percentage completion (α) at equilibrium was estimated at 25% (10 fold α-CD) and 77% (100 fold α-CD), respectively. Consequently, the ratio of complexed to un-complexed **rac-2** is only *ca.* 3-fold more at the higher cyclodextrin concentration. Sten Volmer plots were analysed under models including static and dynamic quenching and fractional accessibility for rigour of comparing results. Similar values for Stern-Volmer constants (K_{sv} ~ 1600 M^{-1}) were obtained for all three cases at low $S_2O_8^{2-}$ concentrations. At higher concentrations the fractional accessibility model was more appropriate revealing ground state complexation with the $S_2O_8^{2-}$. It was very noticeable that steady-state luminescence measurements revealed that a 100-fold excess of α-CD partially quenched the emission of both rac-**2** and $[Ru(bpy)_3]^{2+}$. Although the Stern-Volmer experiments do not conclusively rule out a steric hindrance effect for the quenching reaction, it is clear that working at high excess loads of cyclodextrin is counterproductive.

Photostability measurements under reaction conditions

The main interest of the study was to see if the presence of a cyclodextrin would enhance the photostability of the **rac-2** sensitizer under the operating reaction conditions of water oxidation. The reaction studied used the water oxidation catalyst $[Ru^{II}(bda)(4\text{-bromopyridine})_2]$ (**RuCAT)**, where (H_2bda **=** 2,2'-bipyridine-6,6'-dicarboxylic acid), and $S_2O_8^{2-}$ as the sacrificial electron acceptor.[32] In a typical experiment a cuvette containing a 0.1 M phosphate buffer aqueous solution was charged with **RuCAT**, the photosensitizer (**rac-2** or $Ru(bpy)_3^{2+}$, c = 21 μM), $K_2S_2O_8$ and the cyclodextrin; both α-CD and β-CD were tested using a 10-fold excess. Under these conditions for **rac-2** α = 41% (α-CD). The case for β-CD is slightly more convoluted since both 1:1 and 2:1 complexes co-exist in solution. Taking into consideration both the binding constants and conditions α = 23%. Solutions were illuminated using a white LED ring lamp (35 mW cm^{-2}), which was switched off at specific time intervals and UV/visible spectra recorded, after allowing two minutes for the solution to recover the photosensitizer from the photo-generated Ru^{3+} oxidation state. The plots in Figure 4 illustrate the decomposition of the ground-state photosensitizer after passing through several redox cycles over about 20 minutes. Table 2 collates the data of decomposition kinetics for rac-**2** and $Ru(bpy)_3^{2+}$ for comparison. There is a clear enhancement in the stability of rac-**2** by the presence of either cyclodextrin, despite the fact that not all the photosensitizer is in the complexed state. A control experiment where $Ru(bpy)_3^{2+}$ and α-CD or β-CD were used in a 10-fold excess, did not display any enhanced photostability. Reading too much into the disparity between the α-CD and β-CD cases is fraught because of the differences in the degree of complexation. However, the general upward trend is especially encouraging since it follows the increase for the α values. In fact, there is a tentative correlation between k_{obs} and α as illustrated in the insert of Figure 4.

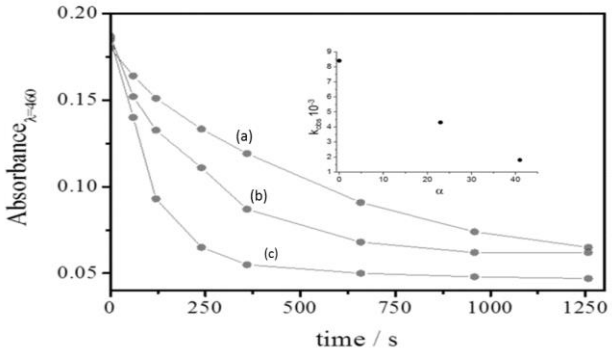

Figure 4. Absorbance at λ_{max} *vs.* time of 2 mL 0.1 M phosphate buffer aqueous solution (pH 7.0) containing 21 μM ***rac*-2**, 10 μM **RuCAT**, 10 mM $K_2S_2O_8$ and 210 μM α–CD (a), 210 μM βCD (b) and without CD (c). Inset: correlation between k_{OBS} and α of each measurement.

Table 2. Summary of the kinetic constants k_{obs} obtained in the absence and presence of CD.

sensitizer	α–CD	β–CD	k_{obs} (10^{-3} s^{-1})[a]
$[Ru(bpy)_3]^{2+}$	-	-	9.3
***rac*-2**	-	-	8.4
$[Ru(bpy)_3]^{2+}$	10 equiv.	-	10.4
***rac*-2**	10 equiv.	-	1.8
***rac*-2**	-	10 equiv.	4.3

[a]From fit to a single exponential of the decay curve.

Oxygen Evolving Studies

Given the favourable thermodynamics for water oxidation by **rac-2**, in the presence of **RuCAT**, the oxygen evolving capability of

the complex was tested. An outgassed aqueous solution of **rac-2** (21 μM), **RuCAT** (10 μM) and $S_2O_8^{2-}$ (10 mM) at pH 7.0 was irradiated under 100 mW cm^{-2} and the oxygen evolution was monitored over time using a calibrated gas-phase Clark-type oxygen electrode. An identical experiment was also carried out in the presence of α-CD (α = 41%). The resulting plots of oxygen formation over time are illustrated in Figure 5. A slightly higher activity is observed with **rac-2** compared to the parent $[Ru(bpy)_3]^{2+}$ given the 20 mV difference in their thermodynamic oxidation potentials. However, most striking is the enhanced formation of oxygen when α-CD was added, improving the turnover (TON) from 62 to 100. As observed in Figure 5, the main difference is that whereas without α-CD the reaction stops after 300 s, the enhanced stability of the photosensitizer by addition of α-CD extends the reaction until *ca.* 500 s. As expected the initial slopes up to *ca.* 200 s for all three cases are identical, since the turnover of oxygen is dependent on **RuCAT**. It is also noted that the increase in TON mirrors satisfactorily the percentage completion (α) for cyclodextrin complexation. Furthermore, we can rule out that the cyclodextrin protects **RuCAT**, since a recent report has shown this is not the case.[16] A control experiment using $[Ru(bpy)_3]^{2+}$, α-CD and the catalyst showed the same activity as without the cyclodextrin (black line in Figure 5) as inferred from the photostability experiments shown in the previous section.

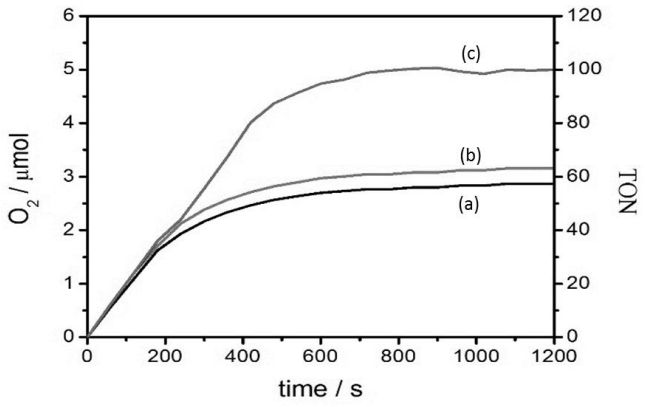

Figure 5. Oxygen evolution profiles (photochemically induced) of 10 μM complex **RuCAT** at pH 7.0 in a 20 mM phosphate solution at 20ºC, upon irradiation with a white LED ring lamp (100 mW cm^{-2}). 10 mM $K_2S_2O_8$ was used as a sacrificial electron acceptor and 21 μM of $Ru(bpy)_3]Cl_2$ (a), ***rac*-2** (b) or ***rac*-2** with 210 μM α-CD (c) as photosensitizer.

Conclusions

By using the concept of directional excited-state electron delocalization we have demonstrated that the protection of a ruthenium(II) bpy-based photosensitizer towards degradation is possible. The partial encapsulation of a molecular fragment on the bipyridine ligand by a cyclodextrin appears to provide shelter under the harsh conditions of water oxidation. The drawback with the current approach, however, is the reliance on bimolecular binding of the cyclodextrin with the photosensitizer. The binding constant is too low to facilitate complete host-guest complexation under the concentration conditions. A potential solution to such a problem is to "stopper" the cyclodextrin onto the protruding arm of the ruthenium-bipyridine complex to form the rotaxane counterpart. The report by Sun *et al.*[16] showed the important role of supramolecular interactions to enhance electron transfer processes, while this work emphasizes that even simple compounds can be used in combination with cyclodextrins to increase the turnover number for oxygen production. A combination of the two ideas may be a way forward to produce supramolecular photocatalysts that are both more stable and more efficient.

Experimental Section

Materials and Instrumentation

Bulk chemicals were purchased at the highest purity possible from Sigma-Aldrich and used as received unless otherwise stated. Tetra-*n*-butylammonium hexafluorophosphate (TBAH) purchased from Sigma-Aldrich was recrystallised several times from methanol and dried thoroughly under vacuum before being stored in a desiccator. Standard solvents were dried by literature methods before being distilled and stored under nitrogen over 4Å molecular sieves. Spectroscopic-grade solvents were used in all fluorescence/absorption-spectroscopy measurements. $[Ru^{II}Cl_2(2,2'\text{-bipyridine})_2]$[33] and $[Ru^{II}(bda)(4\text{-bromopyridine})_2]$ (H_2bda = 2,2'-bipyridine-6,6'-dicarboxylic acid) (**RuCAT**)[32] were synthesized according to reported procedures.

^1H and ^{13}C NMR spectra were recorded with either Bruker AVANCE III 300 MHz, JEOL ECS-400 MHz or Bruker AVANCE III HD 700 MHz spectrometers. Chemical shifts for ^1H and ^{13}C NMR spectra are referenced relative to the residual deuterated solvent. Routine mass spectra and elemental analyses were obtained using in-house facilities.

Absorption spectra were recorded using a Hitachi U3310 spectrophotometer and corrected fluorescence spectra were recorded using a Lambda Advanced F 4500 spectrometer. Photostability measurements were performed using a white LED ring lamp (35 mW cm^{-2}) that illuminated the cuvette containing the photosensitizer, the catalyst (**RuCAT**), $K_2S_2O_8$ as sacrificial electron acceptor and the corresponding cyclodextrin. The lamp was switched off at specific times, the solution was allowed to stand for 2 minutes to avoid the measurement of transient Ru^{3+} species, and a UV-vis spectrum was acquired. The kinetic constant k_{OBS} was obtained from a plot of absorption vs. time that was fitted to a single exponential decay.

Cyclic voltammetry experiments were performed using a fully automated CH Instruments Electrochemical Analyzer and a three electrode set-up consisting of a glassy carbon working electrode, a platinum wire-counter electrode and a sodium saturated calomel reference electrode (SSCE). All studies were performed in deoxygenated CH_3CN containing TBAH (0.1 M) as background electrolyte. The solute concentrations were typically 0.3 mM. Redox potentials were reproducible to within ±15 mV.

ITC experiments: the titration measurements were carried out in an ITC 200 titration calorimeter (MicroCal, GE). Before loading, all the solutions were dyalized and thoroughly degassed. The reference cell was filled with ultra-pure water. Photosensitizer Λ-**2** (1.14 mM) was dissolved in a sodium phosphate buffer (50 mM, pH 7) and was kept in the sample cell. A syringe was filled with the corresponding cyclodextrin dissolved in the same solution. For each titration, 16 injections of 2 μL were performed with an interval of 2 min at 298 K. In a parallel experiment, the heat of dilution was measured by injecting the cyclodextrin solution into the buffer solution without containing the photosensitizer in the sample cell. The experiment data were processed with the Origin software. The reaction heat was determined by subtracting the heat of dilution from the binding experiment. The titration curves were analyzed by using a nonlinear least-square minimization method with an appropriate model.

Photochemical oxygen evolution: Irradiation was carried out with a white LED ring lamp with an intensity of 100 mW cm^{-2}. The temperature of the cell was maintained constant at 20ºC. Oxygen evolution was analyzed with

a gas-phase Clark-type oxygen electrode (Unisense Ox-N needle microsensor). The electrode was calibrated using nitrogen saturated, air saturated and a known amount of oxygen within the range of concentrations obtained in the experiments. In a typical experiment, to 5 mL of 20 mM phosphate buffer solution (pH 7.0) were added 10 μM of **RuCAT**, 21 μM of **rac-2**, 210 μM of α-CD and 10 mM of $K_2S_2O_8$ and were degassed for 10 minutes prior to irradiation.

Synthesis

rac-[Ru(4-Br-bpy)(bpy)$_2$](PF$_6$)$_2$, rac-**1**. [Ru(bpy)$_2$Cl$_2$] (20 mg) and 4-Br-bpy (9.6 mg) were added to 10 mL of an ethanol:water mixture (1:1) in a 25-mL flask. The solution was refluxed for 4 h and cooled to room temperature. A saturated aqueous solution of NH_4PF_6 was added to the reaction mixture, which was concentrated until a precipitate formed. The sample was cooled at 0 °C for 1 h. The solid material was then collected by filtration. The compound was purified by column chromatography on Al_2O_3 from dichloromethane/acetonitrile (3/1); R_f = 0.45. Yield: 80%. Elemental analysis calcd (%) for $C_{30}H_{23}BrF_{12}N_6P_2Ru$: C = 38.40, H = 2.47, N = 8.96; found: C = 38.83, H = 2.03, N = 8.70. ^{1}H-NMR (400 MHz, CD_3CN): δ 8.72 (d; *J* 1.3; 1H; H3); 8.49 (dd; *J* 8.3, 1.9; 5H; H8, H13, H13', H18, H18'); 8.07 (t; *J* 8.0; 5H; H9, H14, H14', H19, H19'); 7.78 (dd; *J* 5.0, 1.2; 1H; H11); 7.73 (dd; *J* 5.4, 1.2; 1H; H16'); 7.70 (d; *J* 5.3; 3H, H16, H21, H21'); 7.56 (m; 2H; H5, H6); 7.44-7.36 (m, 5H, H10, H15, H15', H20, H20'). ^{13}C-NMR (400 MHz, CD_3CN): δ 157.8, 153.1 (C6), 152.7 (C11), 152.6 (C16, C16', C21, C21'), 138.8 (C9, C14, C14', C19, C19'), 131.4 (C5), 129.0 (C3), 128.5 (C10, C15, C15', C20, C20'), 125.7 (C8), 125.2 (C13, C13', C18, C18'). ESI-MS: *m/z* calcd for $C_{30}H_{23}BrN_6Ru$ 324.0102 $[M/2]^{2+}$, found 324.0099; 792.9853 $[M+PF_6]^+$, found 792.9888.

rac-[Ru(Ph-*E*-bpy)(bpy)$_2$](PF$_6$)$_2$, rac-**2**. [Ru(bpy)$_2$Cl$_2$] (40 mg) and Ph-*E*-bpy (21 mg) were added to 10 mL of an ethanol:water mixture (1:1) in a 25-mL flask. The solution was refluxed for 4 h and cooled to room temperature. A saturated aqueous solution of NH_4PF_6 was added to the reaction mixture, which was concentrated until a precipitate formed. The sample was cooled at 0 °C for 1 h. The solid material was then collected by filtration. The compound was purified by preparative thin chromatography on SiO_2 from dichloromethane/acetonitrile (4/1); R_f = 0.90. Yield: 75%. Elemental analysis calcd (%) for $C_{38}H_{28}F_{12}N_6P_2Ru$: C = 47.56, H = 2.94, N = 8.76; found: C = 48.94, H = 3.11, N = 8.15. ^{1}H-NMR (400 MHz, CD_3CN): δ 8.61 (s; 1H; H3); 8.53 (d; *J* 7.4; 1H; H8); 8.51 (d; *J* 8.0; 4H; H21, H21', H26, H26'); 8.07 (t; *J* 7.8; 5H, H9, H22, H22', H27, H27'); 7.79 (d; *J* 5.4; 1H; H11); 7.74 (d; *J* 5.9; 1H; H6); 7.72 (d; *J* 5.8; 4H: H24, H24', H29, H29'); 7.61 (d; *J* 8.0; 2H, H15, H19); 7.51 (t; *J* 5.0; 1H; H17); 7.50 (t; *J* 7.0; 2H; H16, H18); 7.45-7.38 (m; 6H; H5, H10, H23, H23', H28, H28'). ^{13}C-NMR (400 MHz, CD_3CN): δ 158.2 (C7), 157.8 (C20, C20', C25, C25'), 157.1 (C2), 152.7 (C11), 152.6 (C6), 152.5 (C24, C24', C29, C29'), 138.8 (C9, C22, C22', C27, C27'), 133.2 (C15), 133.0 (C19), 131.2 (C17), 130.0 (C16, C18), 129.5 (C5), 128.8 (C10), 128.6 (C23, C23', C28, C28'), 126.7 (C3), 125.4 (C8), 125.2 (C21, C21', C26, C26'), 122.0 (C14), 98.5 (C13), 86.3 (C12). ESI-MS: *m/z* calcd for $C_{38}H_{28}N_6Ru$ 335.0709 $[M/2]^{2+}$, found 335.0678; 815.1061 $[M+PF_6]^+$, found 815.1069.

Δ-[Ru(Br-bpy)(bpy)$_2$](PF$_6$)$_2$, Δ-**1a**. Δ-[Ru(bpy)$_2$(py)][(+)-*O,O*'-dibenzoyl-D-tartrate]•12H$_2$O (45 mg) and 4-bromo-bipyridine (9.3 mg) were added to 2 mL of ethylene glycol (10% water) in a 10-mL flask. The solution was heated to 120 °C for 4 h, cooled to room temperature, and diluted with 2 mL of H_2O. The resultant mixture was then filtered. A saturated aqueous solution of NH_4PF_6 was added dropwise to the filtrate until no more precipitate formed. The solid material was then collected by filtration. The compound was purified by preparative TLC on SiO_2 from dichloromethane/acetonitrile (4/1); R_f = 0.67; Yield = 65%.

Λ-[Ru(Br-bpy)(bpy)$_2$](PF$_6$)$_2$, Λ−**1b**. The complex was prepared in the same way as the Δ form described above using the chiral building block Λ-[Ru(bpy)$_2$(py)$_2$][(-)-*O,O*'-dibenzoyl-D-tartrate]•12H$_2$O; R_f = 0.67; Yield: 62%.

Δ-[Ru(Ph-*E*-bpy)(bpy)$_2$](PF$_6$)$_2$, Δ-**2a**. The complex was prepared using the chiral building block Δ-[Ru(bpy)$_2$(py)$_2$][(+)-*O,O*'-dibenzoyl-D-tartrate]•12H$_2$O and 4-(phenylethynyl)-bipyridine (9.5 mg). The compound was purified by preparative TLC on SiO_2 from dichloromethane/acetonitrile (4/1); R_f = 0.83; Yield = 58%.

Λ-[Ru(Ph-*E*-bpy)(bpy)$_2$](PF$_6$)$_2$, Λ-**2b**. The complex was prepared in the same way as the Δ form described above using the chiral building block Λ-[Ru(bpy)$_2$(py)$_2$][(-)-*O,O*'-dibenzoyl-D-tartrate]•12H$_2$O; R_f = 0.83; Yield = 61%.

Acknowledgements

P.F. gratefully acknowledges the Royal Society for the Newton Fellowship and for the financial support. We also thank the Engineering and Physical Sciences (EPSRC) sponsored Mass Spectrometry at Swansea for the collection of mass spectra. Chris Johnson is acknowledged for his support in the ITC measurements.

Keywords: photosensitizer • photooxidation • ruthenium • cyclodextrin • chirality

[1] O. Kohle, M. Grätzel, A. F. Meyer, T. B. Meyer, T. B. *Adv. Mater.* **1997**, *9*, 904-906.
[2] Y. Qin, Q. Peng, *Int. J. Photoenergy* **2012**, DOI://10.1155/2012/291579.
[3] A. Hagfeldt, G. Boschloo, L. Sun, L. Kloo, H. Pettersson, *Chem. Rev.* **2010**, *110*, 6595-6663.
[4] J. Wu, Z. Lan, J. Lin, M. Huang, Y. Huang, L. Fan, G. Luo, *Chem. Rev.* **2015**, *115*, 2136-2173.
[5] P. Farràs, C. Di Giovanni, J. N. Clifford, E. Palomares, A. Llobet, *Coord. Chem. Rev.* **2014**, DOI://10.1016/j.ccr.2014.10.007.
[6] Z. Yu, F. Li, L. Sun, *Energ. Environ. Sci.* **2015**, *8*, 760-775.
[7] H. C. Chen, D. G. Hetterscheid, R. M. Williams, J. I. van der Vlugt, J. N. Reek, A. M. Brouwer, *Energ. Environ. Sci.* **2015**, *8*, 975-982.
[8] R. Bofill, J. García-Antón, L. Escriche, X. Sala, *J. Photoch. Photobio. B* **2014**, DOI://10.1016/j.jphotobiol.2014.10.022.
[9] P. Farràs, A. C. Benniston, *Tetrahedron Lett.* **2014**, *55*, 7011-7014.
[10] N. Kaveevivitchai, R. Chitta, R. Zong, M. El Ojaimi, R. P. Thummel, *J. Am. Chem. Soc.* **2012**, *134*, 10721–10724.
[11] E. Arunkumar, C. C. Forbes, B. D. Smith, *Eur. J. Org. Chem.* **2005**, 4051-4059.
[12] D. J. Wood, F. E. Hrùska, W. Saenger, *J. Am. Chem. Soc.* **1977**, *99*, 1735-1740.
[13] F. Cramer , W. Saenger , H.-Ch. Spatz , *J. Am. Chem. Soc.* **1967**, *89*, 14-20.
[14] a) E. Adar, Y. Degani, Z. Goren, I. Willner, *J. Am. Chem. Soc.* **1986**, *108*, 4696-4700; b) K. Tennakone, G. R. R. A. Kumara, A. R. Kumarasinghe, P. M. Sirimanne, *J. Photoch. Photobio. A* **1996**, *96*, 167-169; c) N. Mourtzis, P. C. Carballada, M. Felici, R. J. Nolte, R. M. Williams, L. de Cola, M. C. Feiters, *Phys. Chem. Chem. Phys.* **2011**, *13*, 7903-7909.
[15] K. J. Balkus Jr, A. G. Gabrielov, in *Inclusion Chemistry with zeolites: nanoscale materials by design*, Springer, Netherlands, **1995**, pp. 159-184.
[16] H. Li, F. Li, B. Zhang, X. Zhou, F. Yu, L. Sun, *J. Am. Chem. Soc.* **2015**, *137*, 4332-4335.
[17] A. Harriman, A. Khatyr, R. Ziessel, *Phys. Chem. Chem. Phys.*, **1999**, 1, 4203-4211.
[18] A. C. Benniston, V. Groshenny, A. Harriman, R. Ziessel, *Angew. Chem. Int. Ed. Engl.* **1994**, 33, 1884-1885.
[19] P. K. Ghosh, B. S. Brunschwig, M. Chou, C. Creutz, N. Sutin, *J. Am. Chem. Soc.* **1984**, *106*, 4772-4783.
[20] X. Hua, A. Von Zelewsky, *Inorg. Chem.* **1995**, *34*, 5791-5797.
[21] B. P. Sullivan, D. J. Salmon, T. J. Meyer, *Inorg. Chem.* **1978**, *17*, 3334-3341.

[22] Md. M. Ali, F. M. Mac-Donnell, *J. Am. Chem. Soc.* **2000**, *122*, 11527 11528.
[23] E. C. Constable, P. Harverson, C. E. Housecroft, E. Nordlander, J. Olsson, *Polyhedron* **2006**, *25*, 437-458.
[24] A. L. Thakkar, P. V. Demarco, *J. Pharm. Sci.* **1971**, *60*, 652–653.
[25] D. Greatbanks, R. Pickford, *Magn. Reson. Chem.* **1987**, *25*, 208-215.
[26] T. Aree, J. Jacob, W. Saenger, H. Hoier, *Carbohydr Res.* **1998**, *307*, 191-197.
[27] Y. Shu, Z. S. Breitbach, M. K. Dissanayake, S. Perera, J. M. Aslan, N. Alatrash, F. M. MacDonell, D. W. Armstrong, *Chirality* **2015**, *27*, 64-70.
[28] A. Börje, O. Köthe, A. Juris, *J. Chem. Soc. Dalton* **2002**, 843-848.
[29] A. A. Vlcek, E. S. Dodsworth, W. J. Pietro, A. B. P. Lever, *Inorg. Chem.* **1995**, *34*, 1906-1913.
[30] E. Galoppini, W. Guo, W. Zhang, P. G. Hoertz, P. Qu, G. J. Meyer, *J. Am. Chem. Soc.* **2002**, *124*, 7801-7811.
[31] A. Lewandowska-Andralojc, D. E. Polyansky, *J. Phys. Chem. A* **2013**, *117*, 10311-10319.
[32] L. Duan, L. Wang, A. K. Inge, A. Fischer, X. Zou, L. Sun, *Inorg. Chem.* **2013**, *52*, 7844-7852.
[33] B. P. Sullivan, D. J. Salmon, T. J. Meyer, *Inorg. Chem.* **1978**, *17*, 3334-3341.